PRIMARY RESEARCH ARTICLE

Global Change Biology WILEY

The CO_2-equivalent balance of freshwater ecosystems is non-linearly related to productivity

Charlotte Grasset[1] (iD) | Sebastian Sobek[1] | Kristin Scharnweber[1] | Simone Moras[1] | Holger Villwock[1] | Sara Andersson[1] | Carolin Hiller[1] | Anna C. Nydahl[1] | Fernando Chaguaceda[1] | William Colom[2] | Lars J. Tranvik[1]

[1]Limnology, Department of Ecology and Genetics, Uppsala University, Uppsala, Sweden

[2]Erken Laboratory, Department of Ecology and Genetics, Uppsala University, Uppsala, Sweden

Correspondence
Charlotte Grasset, Limnology, Department of Ecology and Genetics, Uppsala University, Uppsala, Sweden.
Email: charlottemjgrasset@gmail.com

Present address
Holger Villwock, SLU, Department of Aquatic Sciences and Assessment, Swedish University of Agricultural Sciences, Uppsala, Sweden
Carolin Hiller, Department of Hydrology, Bayreuth Center of Ecology and Environmental Sciences, University of Bayreuth, Bayreuth, Germany

Funding information
Swedish Research Council, Grant/Award Number: 2018-04524 and 2017-00635; Knut och Alice Wallenbergs Stiftelse, Grant/Award Number: 2013.0091; European Research Council, Grant/Award Number: 336642

Abstract

Eutrophication of fresh waters results in increased CO_2 uptake by primary production, but at the same time increased emissions of CH_4 to the atmosphere. Given the contrasting effects of CO_2 uptake and CH_4 release, the net effect of eutrophication on the CO_2-equivalent balance of fresh waters is not clear. We measured carbon fluxes (CO_2 and CH_4 diffusion, CH_4 ebullition) and CH_4 oxidation in 20 freshwater mesocosms with 10 different nutrient concentrations (total phosphorus range: mesotrophic 39 μg/L until hypereutrophic 939 μg/L) and planktivorous fish in half of them. We found that the CO_2-equivalent balance had a U-shaped relationship with productivity, up to a threshold in hypereutrophic systems. CO_2-equivalent sinks were confined to a narrow range of net ecosystem production (NEP) between 5 and 19 mmol O_2 m^{-3} day^{-1}. Our findings indicate that eutrophication can shift fresh waters from sources to sinks of CO_2-equivalents due to enhanced CO_2 uptake, but continued eutrophication enhances CH_4 emission and transforms freshwater ecosystems to net sources of CO_2-equivalents to the atmosphere. Nutrient enrichment but also planktivorous fish presence increased productivity, thereby regulating the resulting CO_2-equivalent balance. Increasing planktivorous fish abundance, often concomitant with eutrophication, will consequently likely affect the CO_2-equivalent balance of fresh waters.

KEYWORDS

carbon dioxide, eutrophication, food web structure, greenhouse gas, methane, oxidation

1 | INTRODUCTION

Freshwater ecosystems are important components of the global carbon (C) cycle (Cole et al., 2007; Tranvik et al., 2009). They have a significant effect on the atmospheric fluxes of the greenhouse gases (GHGs) carbon dioxide (CO_2) and methane (CH_4;

Bastviken, Tranvik, Downing, Crill, & Enrich-Prast, 2011; Raymond et al., 2013) and also bury C in their sediments, which removes C from the active C cycle (Mendonça et al., 2017). The overall contribution to atmospheric GHG concentrations (Prairie et al., 2018) can be quantified using the CO_2-equivalent balance, which accounts for the difference in global warming potential of CO_2 (GWP = 1) and

CH_4 (GWP = 34, at 100 years timescale including climate-carbon feedbacks; Myhre et al., 2013).

While several factors drive CO_2 emission from fresh waters (Maberly, Barker, Stott, & De Ville, 2013; Marcé et al., 2015), many fresh waters are net heterotrophic ecosystems due to import and subsequent mineralization of terrestrial organic matter. Hence, they are net sources of atmospheric CO_2 (Cole, Pace, Carpenter, & Kitchell, 2000; Duarte & Prairie, 2005; Pace et al., 2004; CO_2 emissions > 0). With increasing inorganic nutrient supply and thus productivity, net ecosystem metabolism turns to become net autotrophic (Hanson, Bade, Carpenter, & Kratz, 2003; Hanson et al., 2004), thus CO_2 emissions are expected to decrease (Balmer & Downing, 2011; Pacheco, Roland, & Downing, 2013; Schindler, Carpenter, Cole, Kitchell, & Pace, 1997), C burial to increase (Anderson, Bennion, & Lotter, 2014; Flanagan, Mccauley, & Wrona, 2006; Heathcote & Downing, 2012) and ecosystems can turn into CO_2 sinks (Balmer & Downing, 2011; CO_2 emissions < 0).

However, eutrophication can change the CO_2-equivalent balance by methanogenic microbes in the sediments transforming a fraction of the CO_2 fixed by autochthonous primary production into CH_4 (Grasset et al., 2018; West, Coloso, & Jones, 2012). Accordingly, CH_4 emissions have been shown to increase exponentially with freshwater productivity (Bastviken, Cole, Pace, & Tranvik, 2004; Beaulieu, DelSontro, & Downing, 2019; Davidson et al., 2018; Grasset, Abril, Guillard, Delolme, & Bornette, 2016). Eutrophication consequently has two opposite effects on the CO_2-equivalent fluxes, inducing both increased CO_2 uptake from the atmosphere, but also enhanced CH_4 release to the atmosphere (DelSontro, Beaulieu, & Downing, 2018). However, the effect of productivity on the overall CO_2-equivalent balance of freshwater ecosystems is rarely considered. The only study published to date reports a negative effect of productivity on the CO_2-equivalent emission of shallow-water mesocosms (Davidson et al., 2015), but did not measure CH_4 emission via bubbles (ebullition), which typically is a major CH_4 emission pathway (Bastviken et al., 2004; Davidson et al., 2018), and was further comprised of only two levels of productivity. This study could as such not answer the question of how far a shift in ecosystem productivity, which is the typical situation in natural systems (Rineau et al., 2019), may affect the CO_2-equivalent balance.

Autochthonous primary production in fresh waters is not only controlled by inorganic nutrient supply but also by food web structure (Carpenter et al., 2001). Animals often have indirect effects on biogeochemical processes, sometimes with a large impact on GHG emissions (Schmitz et al., 2014). For instance, increasing planktivorous fish abundance, often concomitant to eutrophication (Jeppesen, Peder Jensen, SØndergaard, Lauridsen, & Landkildehus, 2000; Moss et al., 2011), can increase primary production and thus CO_2 uptake by photosynthesis by reducing grazing pressure from zooplankton (Atwood et al., 2013; Cole et al., 2000; Schindler et al., 1997). On the other hand, fish may reduce CH_4 emission from fresh waters through top-down control of zooplankton that graze on CH_4 oxidizers (Devlin, Saarenheimo, Syväranta, & Jones, 2015). The overall effect

of food web structure on the CO_2-equivalent balance of freshwater ecosystems has not yet been investigated.

Only a fraction of the CH_4 that is produced in anoxic sediments reaches the atmosphere, primarily due to aerobic CH_4 oxidation by CH_4-oxidizing bacteria. Between 45% and 100% of the produced CH_4 in lake sediments could be lost by oxidation (Bastviken, 2009), mainly during CH_4 transport by diffusion across the oxic-anoxic interface in the sediment or in the water column. Recent studies show that the responses to drivers such as temperature and nutrients are different for CH_4 production and CH_4 oxidation (Fuchs, Lyautey, Montuelle, & Casper, 2016; Sepulveda-Jauregui et al., 2018). This implies that the balance between CH_4 oxidized and CH_4 produced, and thus the proportion of the produced CH_4 that is emitted by diffusion to the atmosphere might change along environmental and climatic gradients. Accordingly, the CO_2-equivalent balance of fresh waters may vary in complex ways across productivity gradients in response to the combined effects of CO_2 fixation and mineralization, food web effects, and production as well as oxidation of CH_4.

To determine how the CO_2-equivalent balance depends on productivity, we set up a total of 20 mesocosms, two at each of the 10 nutrient levels (total phosphorus [TP] from 39 to 939 μg/L), and one at each nutrient level was stocked with fish. We hypothesized that CH_4 emission will increase exponentially and CO_2 will decrease linearly with productivity, such that the CO_2-equivalent emission will have a minimum along a productivity gradient. In addition, we hypothesized that the presence of fish reduces emissions of CO_2 and CH_4 due to reduction of zooplankton grazing on phytoplankton and CH_4 oxidizers.

2 | MATERIALS AND METHODS

2.1 | Mesocosm setup

Twenty white opaque high density polyethylene mesocosms of 2 m height and 1 m diameter were deployed in the mesotrophic hard water lake Erken (59°51′N, 18°36′E, Sweden). The mesocosms were filled on June 2017 up to 1.65 m with c. 1,200 L of Erken water filtered through a 200

μm mesh (to remove large plankton and algal colonies), and about 80 L of surface sediment sampled from Erken at 15 m depth 1 week before. TP and total nitrogen (TN) concentration were set to 10 different levels, and of the two mesocosms receiving the same nutrient addition, one mesocosm was stocked with two juvenile crucian carp (*Carassius carassius*) individuals, which reflects the crucian carp density of natural populations (Holopainen & Pitkänen, 1985). The diet of juvenile crucian carp consists of zooplankton and Chrionomidae (Penttinen & Holopainen, 1992), and they were therefore expected to exert the hypothesized top-down control on zooplankton abundance and grazing. The experiment was run for 1 year and 3 months to allow for new detritus to deposit on the sediment and thus affect methanogenesis. Zooplankton inoculates (approximately 13 individuals L^{-1}), obtained from tows with a 100 μm plankton net were added to the mesocosms.

Fish were added to 10 of the mesocosms during spring and summer (July–October 2017 and May–September 2018) and were removed during winter by hand-netting in order to avoid death because of low oxygen during ice cover. The mesocosms were shaded with black plastic sheets placed on the outside of walls to limit periphyton growth. In order to allow for all autochthonous organic carbon to reach the sediment and contribute to methanogenesis, the mesocosm walls were scraped every 4 weeks during the ice-free period to detach periphyton. Primarily the fluxes measured during summer 2018 (May–September 2018) were analyzed in this study since there was a lag in the emergence of sediment methanogenesis, which was very low during the first year (2017). However, fluxes and partial pressure of CO_2 and CH_4 throughout the entirety of the experiment (July 2017 to September 2018) are presented in Figures S1–S4 in the Supplementary material.

2.2 | Nutrient gradient establishment

A gradient of TP concentration in the water column with 10 different levels was set: background TP concentration of lake Erken (no addition), 40, 60, 80, 100, 150, 200, 400, 600, and 1,000 µg/L, spanning from mesotrophic to hypereutrophic. Each target concentration was set for two mesocosms, and one mesocosm was stocked with fish during the ice-free period, while the other mesocosm was without fish. TN concentrations were calculated to obtain an N/P atomic ratio of 16, allowing other algae than N-fixing bacteria to colonize the mesocosms (TN target concentration between 0.45 and 11.29 mg/L). Monopotassium phosphate (KH_2PO_4) and ammonium nitrate (NH_4NO_3) were added to adjust to the TP and TN target concentrations on the first day, every 2 weeks during the ice-free period, and every 4 weeks during the ice-covered period. No nutrients were added in the lowest nutrient treatment to keep the background concentration. Over summer 2018, the mean TP values varied between 39 ± 35 (SD) µg/L for the no addition treatments and 939 ± 381 (SD) µg/L for the highest nutrient treatments. An extremely high TP value of 1,000 µg/L can be encountered in fresh waters and it is consequently appropriate to include it in our eutrophication gradient to cover the most extreme cases of eutrophication (DelSontro et al., 2018).

2.3 | Water analyses

Water samples were taken from each mesocosm every 2 weeks during the ice-free period, every 4 weeks otherwise, for nutrient and dissolved organic carbon (DOC) analyses. Water was collected with a 1 m long plastic tube to get integrative samples of the water column. TP concentration was measured using the ammonium molybdate spectrometric method (Swedish standard method SS-EN ISO 6878:2005, Erken Laboratory). TN and DOC concentrations were measured on GF/F filtered (effective pore size 0.7 µm, Whatman®, GE Healthcare) and acidified samples (Hydrochloric acid HCl 1 M) with a Shimadzu TOC-L TNM-L analyzer. Turbidity, pH, temperature, dissolved oxygen, and Chlorophyll a (Chla), were conjointly measured

with a multiprobe (EXO2 Multiparameter Sonde, YSI) at 50, 100 and 125 cm below the water surface. In addition, dissolved oxygen was automatically measured every 10 min with oxygen probes (mini-DO2T PME) at a depth of 25–30 cm below water surface.

2.4 | Zooplankton sampling

Zooplankton samples were taken from the integrated water sample used for the water analyses. Five liters of water was filtered through 55 µm and zooplankton was immediately preserved with Lugol's solution and later analyzed using an inverted microscope (Leica DM IL LED, Leica) with image analysis software (Image Pro Plus version 7.0 for Windows, Media Cybernetics Inc.). Subsamples were counted until reaching 200 individuals and zooplankton were grouped into Cladocera (*Bosmina* sp., *Daphnia* sp., *Ceriodaphnia* sp., *Diaphanosoma* sp., *Polyphemus* sp. and *Scapholeberis* sp.) and Copepoda (Cyclopoida and Calanoida). We measured the total length of up to 20 individuals of each zooplankton taxon using an image analysis software (Image Pro Plus version 7.0 for Windows, Media Cybernetics) to calculate zooplankton biomass based on published length–weight relationships (McCauley, 1984).

2.5 | Primary producer biomass

Phytoplankton biomass was calculated from the Chla (µg/L) measurements in the water column by assuming a C:Chla ratio of 40 (g:g; Lorenzen, 1968). Periphyton biomass was measured using plastic strips, made of the same material as the mesocosms, that were attached to the walls of the mesocosms and reached the full depth down to the sediment. The strips were scraped every 4 weeks during the ice-free period, and biomass was upscaled from the width of the strip (7 cm) to the full diameter of the mesocosm. Samples were dried at 50–60°C, grinded manually into a fine powder with a mortar and a pestle, acidified with HCl 5% and encapsulated in tin capsules for total organic carbon and nitrogen analysis with a C/N elemental analyzer (Costech Analytical Technologies Inc.). The total primary producer biomass in the mesocosms (g C mesocosm^{-1}) was calculated by summing periphyton and phytoplankton biomass. Sediment was sometimes also visibly present on the periphyton strips and thus increased the overall estimation of periphyton C content. However, this contamination was likely to be similar among treatments and negligible for high nutrient treatments since sediment C content was low (7% wt, data not shown) in comparison to periphyton C content (algal C content is typically around 20%–50% wt).

2.6 | Net ecosystem production

Dissolved oxygen automatic measurements at 10 min intervals were used to estimate net ecosystem production (NEP in mg O_2 L^{-1} hr^{-1}) according to Cole et al. (2000) as follows:

$$NEP_t = (DO_t - DO_{t-1}) / \Delta t - \text{air water exchange}, \quad (1)$$

with DO the dissolved O_2 concentration in mg/L and air water exchange in mg O_2 L^{-1} hr^{-1}:

$$\text{Air water exchange} = K_T \times (DO_{sat} - DO_t) / z, \quad (2)$$

z the mixing depth of the system was assumed to be the total water depth (1.65 m) as no stratification was observed in the mesocosms.

DO_{sat} in mg/L was defined according to Benson and Krause Jr. (1984):

$$DO_{sat} = \exp \left(-139.34411 + 1.575701 \times 10^5 \times T^{-1} - 6.642308 \times 10^7 \right.$$
$$\left. \times T^{-2} + 1.2438 \times 10^{10} \times T^{-3} - 8.621949 \times 10^{11} \times T^{-4} \right), \quad (3)$$

with T in Kelvin.

K_T the gas transfer velocity of O_2 in m/hr was calculated from an average K_{600} of 0.014 m/hr measured over summer 2016 and 2017 (details on the gas transfer velocity calculation are given in the supplementary material) as follows:

$$K_T = K_{600} \times (600/Sc)^n, \quad (4)$$

with Sc the Schmidt number of O_2 according to Wanninkhof (1992). We chose $n = 1/2$ since the water surface in the mesocosms was often not smooth.

NEP is expressed in mmol O_2 m^{-3} day^{-1} in the rest of the manuscript for comparisons with literature.

2.7 | CO_2 and CH_4 diffusive fluxes

CH_4 and CO_2 concentrations in the water were measured every 2 weeks during the ice-free period, and every 4 weeks during ice cover, with the headspace method (Cole & Caraco, 1998), by sampling 30 ml of surface water in each mesocosm and equilibrating 1 min with 10 ml of atmospheric air. The gas samples were then transferred to another syringe and analyzed within 24 hr with a gas chromatograph equipped with a flame ionization detector (Agilent Technologies, 7890 A GC system). CO_2 and CH_4 concentrations were calculated from their concentrations in the headspace, the volume of water, and the specific gas solubility of CO_2 (Weiss, 1974) and CH_4 (Yamamoto, Alcauskas, & Crozier, 1976). The diffusive fluxes of CO_2 and CH_4 from the water to the atmosphere were calculated according to Cole and Caraco (1998):

$$F = K_T \times (C - P_{sat} \times K_H), \quad (5)$$

where F is the flux in mmol m^{-2} day^{-1}, K_T is the gas transfer velocity in m/day calculated according to Equation (4), C is the gas concentration

in µmol/L, P_{sat} is the atmospheric gas concentration in µatm and K_H is Henry's constant in mol L^{-1} atm^{-1}.

Daily CO_2 and CH_4 fluxes over summer 2018 were estimated from single daytime measurements in water sampled between 9 a.m. and 11 a.m. Over summer 2017, however, CO_2 concentration was also measured at night (between 3 a.m. and 5 a.m.) at three dates (August, September and October), and the nighttime concentrations of CO_2 were found to be very close to the daytime concentrations measured between 9 a.m. and 11 a.m. (for the three dates, average of the slope = 1.1 and average of the R^2 = .86, data not shown). In May, June and July, the nights are very short (<6 hr) and not completely dark at this latitude, which probably limits the daily variation in CO_2. We consequently assumed that daily variation in CO_2 concentration was low over summer and that a single CO_2 concentration measurement can be representative of its daily concentration.

2.8 | CH_4 ebullitive flux

Bubble traps consisting of a 50 ml syringe standing just below the water surface and attached to 20 cm wide inverted funnel (Davidson et al., 2018; Huttunen, Lappalainen, Saarijärvi, Väisänen, & Martikainen, 2001) were used to collect CH_4 bubbles. The transparent syringes were covered by an opaque light-grey cap to prevent biofilm growth on the surface of the syringe and were cleaned at each sampling. The bubble traps remained permanently in the mesocosms and were sampled every 2 weeks during the ice-free period, every 4 weeks otherwise, when gas was visibly accumulating in the bubble traps. The gas was transferred to a syringe and analyzed within 24 hr with the gas chromatograph. The ebullitive flux of CH_4 (in mmol m^{-2} day^{-1}) was calculated as the amount of CH_4 (mmol) divided by the surface of the funnel in m^2 and the number of days between two consecutive measurements. The volume of the trapped gas exceeded the volume of the syringe at one occasion for mesocosm I with fish (13/06/18) and mesocosm I without fish (14/08/18; A being the lowest nutrient treatment and J the highest), resulting in an underestimation of ebullition flux for these two treatments.

2.9 | CO_2-equivalent balance

CH_4 diffusive as well as CH_4 ebullitive fluxes were converted in CO_2-equivalent (and reported in mg CO_2 m^{-2} day^{-1}) by assuming that 1 g of CH_4 has 34 times the GWP of 1 g of CO_2 for 100 years. This number of 34 includes climate-carbon feedback (Myhre et al., 2013). The sum of ebullitive and diffusive CH_4 fluxes is referred as total CH_4 emissions in the rest of the manuscript. The powerful GHG nitrous oxide (N_2O) was not included in the CO_2-equivalent balance, since it was recently estimated to contribute to only 2% of the total CO_2-equivalent emission of global lakes and reservoirs (DelSontro et al., 2018).

2.10 | CH$_4$ oxidation

Two different methods were used to quantify CH$_4$ oxidation, the fraction of the CH$_4$ produced in sediment that was oxidized in situ was calculated from δ^{13}C-CH$_4$ measurements, and the potential CH$_4$ oxidation rate was calculated from aerobic incubation of the mesocosm water. Details on the potential CH$_4$ oxidation rates are given in the supplementary material.

The fraction of CH$_4$ oxidized in situ was calculated from δ^{13}C of CH$_4$ in mesocosm surface water and δ^{13}C of anaerobically produced CH$_4$ in a sediment incubation. δ^{13}C-CH$_4$ in surface water samples was measured at two dates (13/08/18 and 11/09/18) in each mesocosm. CH$_4$ gas samples were obtained with the headspace method by equilibrating 90 ml of surface water with 20 ml of N$_2$ in 120 ml syringes for 2 min. The gas samples were stored in preevacuated 12 ml vials (Soda Glass Vials 819W, Labco Ltd) that were manually flushed and filled with N$_2$ at atmospheric pressure. Details on the anaerobic sediment incubation can be found in the supplementary material.

The fraction of CH$_4$ oxidized can be calculated for an open steady state system ($F_{oxi\,open}$ Equation 6) or for a closed system ($F_{oxi\,closed}$ Equation 7; Bastviken, Ejlertsson, & Tranvik, 2002):

$$F_{oxi\,open} = \frac{\delta^{13}CH_{4,oxidized} - \delta^{13}CH_{4,newly\,formed}}{(\alpha - 1) \times 1,000}, \quad (6)$$

$$\ln(1 - F_{oxi\,closed}) = \frac{\ln(\delta^{13}CH_{4,newly\,formed} + 1,000) - \ln(\delta^{13}CH_{4,oxidized} + 1,000)}{\alpha - 1}. \quad (7)$$

α, the fractionation factor, is assumed to be 1.02 (Bastviken et al., 2002), δ^{13}CH$_{4,oxidized}$ is the δ^{13}C of CH$_4$ in surface water that has undergone oxidation through the sediment and water column, and δ^{13}CH$_{4,newly\,formed}$ the δ^{13}C of CH$_4$ before oxidation. Some studies use δ^{13}C-CH$_4$ measurements from gas bubbles or bottom waters to estimate δ^{13}CH$_{4,newly\,formed}$ (Barbosa et al., 2018; Thottathil, Reis, Giorgio, & Prairie, 2018) but it is then not possible to exclude that oxidation has already occurred in the sediment or during gas transport. We consequently used δ^{13}C of CH$_4$ produced during an anoxic sediment incubation as δ^{13}CH$_{4,newly\,formed}$ (Zhang, Yu, Fan, Ma, & Xu, 2016) to calculate the fraction of anaerobically produced CH$_4$ in the sediment that is oxidized. In an open system at steady state, CH$_4$ production is supposed constant and CH$_4$ as well as the products of CH$_4$ oxidation can leave freely, while in closed systems, CH$_4$ and oxidation products accumulate (Barbosa et al., 2018; Bastviken et al., 2002). The fraction of CH$_4$ oxidized calculated for open systems gave values often >1 (values between 0.77 and 2.86, mean of 1.59) while it gave a mean of 0.78 and values between 0.56 and 0.95 for closed systems (Figure S5). Values often >1 were also reported in floodplains and lakes (Barbosa et al., 2018; Bastviken et al., 2002; Thottathil et al., 2018) suggesting that the assumptions for open systems might not always be valid in natural systems. We consequently chose to use the fraction of CH$_4$ oxidized in closed systems as a conservative measurement of CH$_4$ oxidation in the rest of the manuscript.

2.11 | Statistical analyses

The effects of TP concentration and fish presence on productivity (NEP) and C fluxes (total CH$_4$ and CO$_2$ emissions) and the fraction of CH$_4$ oxidized were tested with analysis of covariance (lm function with fish presence as a categorical variable). The relationships between C fluxes (total CH$_4$ and CO$_2$ emissions, CO$_2$-equivalent balance), the fraction of CH$_4$ oxidized, potential CH$_4$ oxidation rate, productivity (NEP), primary producer biomass and zooplankton biomass were tested with linear first-order regressions and polynomial models (lm function). All models were based on the averages of the C fluxes, NEP and primary producer biomass over summer 2018 for each mesocosm ($n = 20$) because averages were considered more robust and integrative of the whole period, and indicative of the overall treatment effects regardless of any temporal variability. Furthermore, as we did not see any consistent temporal patterns for C fluxes and NEP (Figures S3, S4 and S6), we preferred to choose the simpler models with averages rather than the more complex mixed-effect models that also show a positive effect of productivity on CH$_4$ emissions and a negative effect on CO$_2$ emissions (Table S1). All variables except the fraction of CH$_4$ oxidized and NEP were log-transformed (natural logarithm) before modeling to normalize distributions and decrease the effect of extreme values. Before log-transformation, a constant was added to CO$_2$ emissions, CO$_2$-equivalent balance (180 mg CO$_2$ m^{-2} day^{-1}) and to potential CH$_4$ oxidation rates (1 mg L^{-1} day^{-1}) to make all values positive. For CO$_2$ emissions and CO$_2$-equivalent balance, the minimum values were −175 and −168 mg CO$_2$ m^{-2} day^{-1}, respectively, the addition of 180 was chosen to give the best data normalization (according to Shapiro tests and histogram plots of the data). The accuracy of the models was assessed by visualizing the residuals and the observed against predicted data. When comparing several polynomial models, the best model was chosen according to the Akaike information criterion. Thresholds of the polynomial model between CO$_2$-equivalent balance and NEP were determined by the "optim" function that returns parameters that minimize a function. All statistical analyses were performed with the R software (R Core Team, 2016).

3 | RESULTS

3.1 | Relationships between C fluxes, productivity and primary producer biomass

As expected, total CH$_4$ emissions (diffusive + ebullitive) increased with productivity while CO$_2$ emissions decreased (Figure 1; Table 1). The increase in total CH$_4$ emissions however, was less pronounced towards the highest productivity values (Figure 1; Table 1). CH$_4$ ebullition also increased with productivity ($p = .004$, $R^2 = .37$) and occurred in 11 out of the 20 mesocosms, for which it contributed in average to 20% (range 0.5%–71.9%) of total CH$_4$ emissions. The CO$_2$-equivalent balance had a U-shaped relationship with productivity
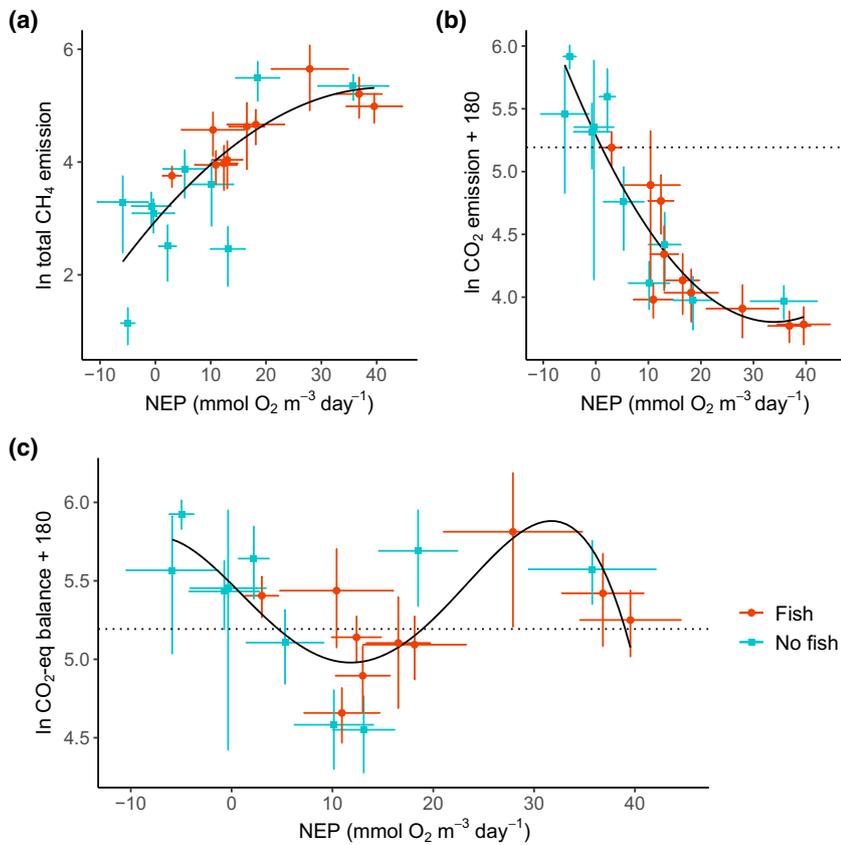
(a)

(b)

(c)

FIGURE 1 Relationships between total CH_4 emissions (a), CO_2 emissions (b) and the CO_2-equivalent balance (c) in mg CO_2 m^{-2} day^{-1} and productivity (net ecosystem production). 180 mg CO_2 m^{-2} day^{-1} is added before log-transformation to CO_2 emissions and the CO_2-equivalent balance to make values strictly positive. See Table 1 for the statistics of the linear and polynomial regressions (black lines). The red points refer to the treatments with fish addition ($n = 10$) and the green points correspond to the treatments without fish ($n = 10$). Error bars represent standard errors. The dotted line corresponds to C fluxes = 0

	Predictor	F	Coefficient	p-value	R^2 (p-value of the model)
Ln total CH_4 emission	NEP	31	0.114	<.0001	.66 (<.0001)
	NEP^2	2	−0.001	NS (.1)	
Ln total CH_4 emission	Ln TP	7	0.452	.02	.47 (.004)
	Fish	8		.01	
Ln CO_2 emission + 180	NEP	90	−0.088	<.0001	.86 (<.0001)
	NEP^2	15	0.001	.001	
Ln CO_2 emission + 180	Ln TP	3	−0.198	NS (.1)	.32 (.04)
	fish	5		.04	
Ln CO_2-eq balance + 180	NEP	0.07	−0.06	NS (.8)	.58 (.008)
	NEP^2	10	−7.35E-04	.006	
	NEP^3	6	2.87E-04	.03	
	NEP^4	4	−5.93E-06	NS (.05)	

TABLE 1 First-order and polynomial regressions between C fluxes (total CH_4 emissions, CO_2 emissions and the CO_2-equivalent balance in mg CO_2 m^{-2} day^{-1}), productivity (NEP in mmol O_2 m^{-3} day^{-1}), and TP (µg/L) with presence of fish as a categorical variable

Note: p-values are given for each predictor (continuous and categorical variables) in the model and coefficients are only given for the continuous variables. In addition, the R^2 and p-value are given for each model. The polynomial models test the multiple linear relationship between NEP and NEP raised at different powers (NEP^2, NEP^3 and NEP^4), and C fluxes. All fluxes are logged (natural logarithm) and a constant is added before log-transformation to make CO_2 emissions and CO_2-equivalent balance positive. All models are performed on averaged values over summer 2018 ($n = 20$, average for 9 dates for C fluxes and 117 dates for NEP). When choosing between different polynomial models, the best model was selected according to the lowest Akaike information criterion.

Abbreviations: NEP, net ecosystem production; NS, not significant.

until a threshold at high productivity (NEP = 32 mmol O_2 m^{-3} day^{-1}) after which the CO_2-equivalent balance decreased again with increasing productivity (Figure 1; Table 1). Eight out of nine mesocosms having NEP values between 5 and 18 mmol O_2 m^{-3} day^{-1} acted as CO_2-equivalent sinks (CO_2-equivalent balance <0) while all mesocosms with higher or lower productivity acted as CO_2-equivalent sources (Figure 1). In accordance with these observations, a polynomial model between the CO_2-equivalent balance and productivity
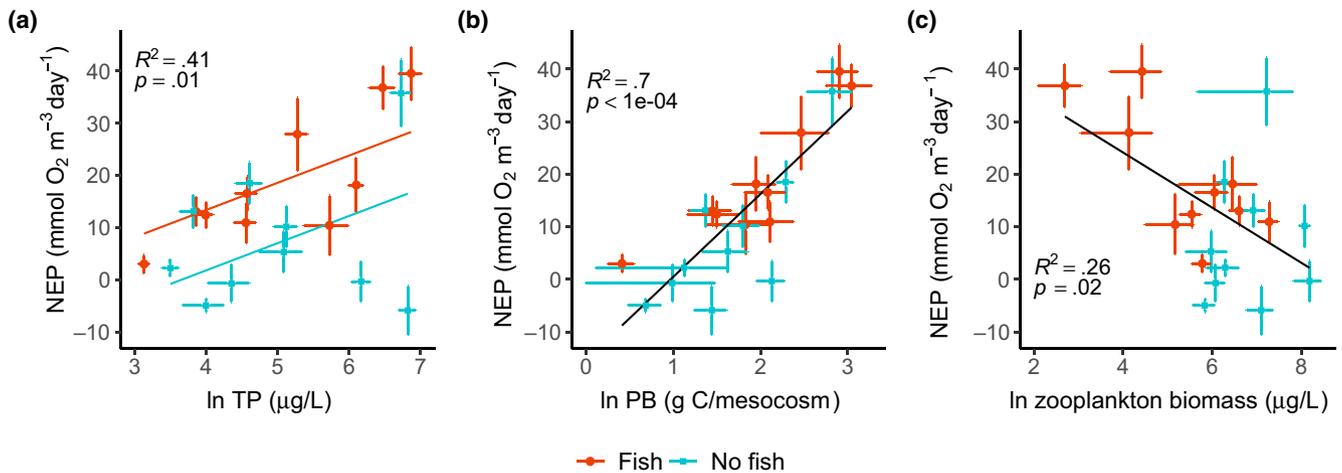
FIGURE 2 Relationship between productivity (net ecosystem production [NEP]) and (a) the average TP concentration over summer 2018, (b) primary producer biomass (PB), and (c) zooplankton biomass. Error bars represent standard errors. Results of the linear regressions (R^2 and p-value of the model) are given in each figure panel. For the regression between NEP and total phosphorus, two lines are drawn, one for the fish (red) and one for the no fish (green) treatments. See Table S2 for more complete statistics

identified two thresholds at NEP = 5 and 19 mmol O_2 m^{-3} day^{-1} at which the mesocosms shifted from source to sink and then back again from sink to source (Figure 1; Table 1).

Productivity was strongly correlated to primary producer biomass (Figure 2; Table S2) and primary producer biomass correlated in similar ways as productivity to total CH_4 and CO_2 emissions and to the CO_2-equivalent balance (Figure S7; Table S3). In the highest productivity treatments, phytoplankton constituted most of the primary producer biomass, and in the other treatments periphyton often dominated (Figure S8).

3.2 | Food web structure and nutrient effect on productivity and C fluxes

Both nutrient concentrations and the presence of fish had a positive effect on primary productivity, thereby regulating CO_2 and CH_4 emissions and the resulting CO_2-equivalent balance (Figure 2; Table S2). The presence of fish induced a trophic cascade and increased productivity through a decrease in zooplankton abundance (Atwood et al., 2013; Schindler et al., 1997; Schmitz et al., 2014; Figure 2; Table S2). Nutrient concentrations and the presence of fish had a positive effect on CH_4 emissions and a negative effect on CO_2 emissions (Table 1; Figure S9). The direct effect of nutrients on CO_2 emissions was however not significant probably because two mesocosms (J and H) with high nutrient concentrations and low productivity had sometimes a high respiration (Figure S9; Figure S4).

3.3 | Relationship between CH_4 oxidation, productivity and food web structure

The fraction of CH_4 that was oxidized increased with productivity (Figure 3) and primary producer biomass, and decreased
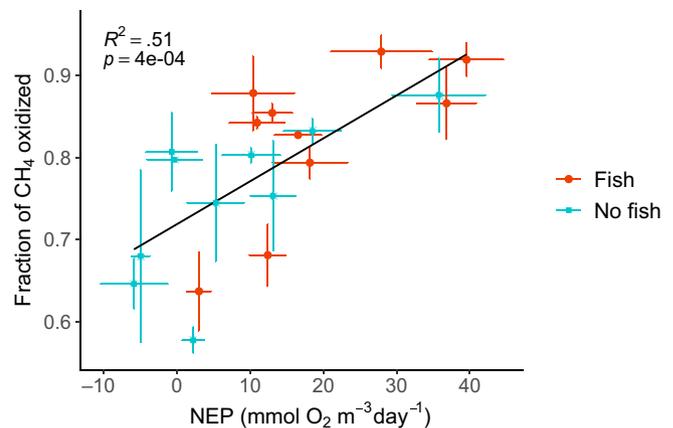

FIGURE 3 Relationships between the fraction of CH_4 oxidized in situ and productivity (net ecosystem production). The results of the linear regression (black line, R^2 and p-value of the model) are directly given in the figure. See Table S4 for more complete statistics. Error bars represent standard errors

with Copepoda biomass (Figure S10; Table S4). However, when CH_4 oxidation was correlated to both fish presence and nutrient concentration, the effect of fish was not significant, suggesting that the presence of fish did not directly enhance CH_4 oxidation (Table S4).

4 | DISCUSSION

Our study is the first to report a non-linear relationship between freshwater productivity (or primary producer biomass) and the net ecosystem CO_2-equivalent balance. This novel result means that eutrophic freshwater ecosystems have the potential to act as CO_2-equivalent sinks, but these sinks are fragile since a small increase or decrease of productivity can turn them again into a

CO_2-equivalent source. We propose a conceptual model describing the non-linear relations between productivity and C fluxes in fresh waters (Figure 4), based on our regressions with NEP (Figure 1). We identified two thresholds at NEP = 5 and 19 mmol O_2 m^{-3} day^{-1} for which the studied freshwater ecosystems shifted from CO_2-equivalent sources to sinks and then returned to being CO_2-equivalent sources. In other fresh waters than the ones studied here, different environmental conditions can shift the thresholds. For example, higher import of dissolved inorganic carbon or higher mineralization of imported organic matter can lead to higher CO_2 emissions (Duarte & Prairie, 2005; Hanson et al., 2004) for the same level of productivity and shift the U-shaped relationship between CO_2-equivalent balance and productivity upwards. In the same way, in temperate and tropical ecosystems higher temperatures can have a positive effect on CH_4 emissions (Davidson et al., 2018; Yvon-Durocher et al., 2014) and are also likely to shift the U-shaped relationship upwards. This implies that the narrow interval of being a CO_2-equivalent sink may be even narrower, and the CO_2-equivalent sink action may disappear completely if the minimum value of CO_2-equivalent balance is positive. Accordingly, we suggest a general pattern of CO_2-equivalent balance across freshwater productivity gradients, shaped by the contrasting effects of productivity on CO_2 and CH_4 fluxes. However, the specific positions of thresholds and the magnitude of the CO_2-equivalent
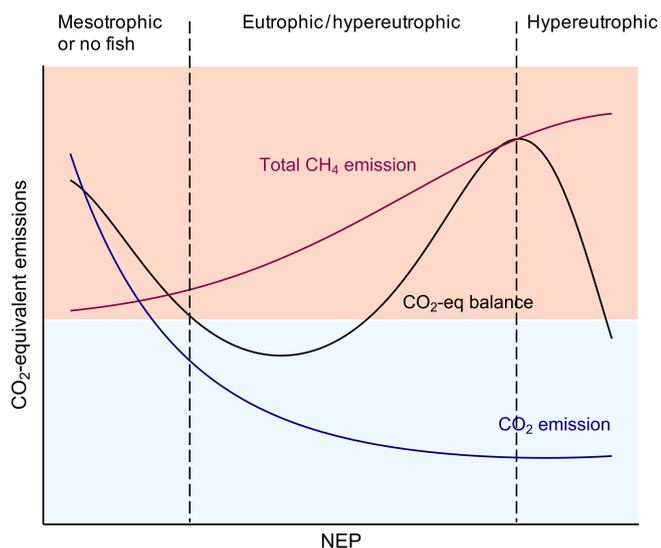

FIGURE 4 Conceptual CO_2-equivalent balance of fresh waters along a productivity gradient. The figure depicts the significant polynomial relationships between C fluxes and productivity, measured in 20 freshwater mesocosms (Table 1). Total CH_4 emissions (diffusive + ebullitive) increased while CO_2 emissions decreased with productivity. CO_2-equivalent balance, calculated as the sum of CH_4 and CO_2 emissions, had a U-shaped relationship with productivity up to a threshold in hypereutrophic systems. The studied freshwater ecosystems acted as CO_2-equivalent sinks within a narrow range of productivity. The range of productivity for which systems can act as CO_2-equivalent sinks is likely to differ, or even disappear for different fresh water types and different climatic zones

emissions is likely to differ among different fresh water types and climate zones. Our findings are not directly applicable to shallow fresh waters colonized by aquatic plants because in addition to providing substrates for CH_4 production, aquatic plants have other complex effects on CH_4 fluxes that would need to be addressed (e.g., CH_4 oxidation in the rhizosphere, CH_4 transport through plant tissues; Davidson et al., 2018; Kosten et al., 2016; Schütz, Schröder, & Rennenberg, 1991). The extent to which the experimentally derived qualitative pattern depicted in Figure 4 manifests quantitatively in various types of lake ecosystems, that is, which levels of productivity represent thresholds of which levels of CO_2-equivalent balance, is therefore unknown and probably variable, and should be the subject of further studies.

Our results indicate that the positive top-down effect of planktivorous fish on productivity decreased CO_2 emissions, in accordance with several studies (Atwood et al., 2013; Cole et al., 2000; Schindler et al., 1997), and increased CH_4 emissions. For CH_4 emissions, this is in apparent contradiction with a recent study showing reduced CH_4 emissions from lakes where fish were present through top-down control of zooplankton that graze on methane oxidizers (Devlin et al., 2015). However, in the latter study the lake was highly rich in humic matter, and the fish addition may not have increased CH_4 production because primary production may have been light-limited in the dark-stained water.

In our study, even if CH_4 emissions increased with productivity, at the same time the fraction of CH_4 oxidized also increased with productivity, hence counteracting CH_4 emissions (Figure 3; Table S4). We consequently attribute the flattening of the increase in total CH_4 emissions and the decrease in CO_2-equivalent balance towards the highest productivity levels (Figure 1) to a higher proportion of CH_4 lost by oxidation in the high-NEP treatments. Several studies indeed showed a flattening or a decrease in CH_4 concentration or CH_4 diffusive emissions towards very high chlorophyll *a* values (i.e., Chl*a* > 200 μg/L; Beaulieu et al., 2019; Wang, Lu, Wang, Yang, & Yin, 2006; Yan et al., 2018). However, very few observations are available for hypereutrophic systems and these patterns should be more thoroughly verified in natural systems.

The increase in the fraction of CH_4 oxidized with productivity cannot be attributed to CH_4 concentration only. Indeed, when the CH_4 concentration is limiting the rate of CH_4 oxidation, it increases linearly with CH_4 concentration (Lofton, Whalen, & Hershey, 2014; Sundh, Bastviken, & Tranvik, 2005), and the fraction of CH_4 oxidized can thus be assumed to be constant. Previous studies have underlined a negative effect of light (Shelley, Ings, Hildrew, Trimmer, & Grey, 2017) or a related positive effect of DOC (Thottathil et al., 2018) on CH_4 oxidation. In our study, the strong correlation between primary producer biomass and the fraction of CH_4 oxidized (Figure S10; Table S4), indicates that light shading by primary producers could enhance CH_4 oxidation. Furthermore, the presence of fish and the associated decrease in zooplankton (Figure 2) could release the grazing pressure on the CH_4 oxidizing bacteria (Devlin et al., 2015), thereby increasing CH_4 oxidation (Figure S10; Table S4), as we hypothesized. Fish

can also directly enhance CH_4 oxidation via sediment reworking (i.e., bioturbation) and increasing O_2 supply to sediment (Oliveira Junior et al., 2019) but this does not seem to be the case in our study because CH_4 oxidation was not significantly correlated to the presence of fish (Table S4). The food web structure and eutrophication had consequently antagonistic effects on CH_4 emissions. Primarily, and most visibly, the presence of fish and nutrient enrichment increased CH_4 emissions via their positive effect on productivity. On the other hand, they also increased CH_4 oxidation most likely via an increase in primary producer biomass and/or a decrease in zooplankton abundance. Importantly, our results suggest that CH_4 oxidation could play an important role for the CO_2-equivalent balance of freshwater ecosystems, calling for more studies on the drivers and magnitude of CH_4 oxidation in natural systems.

We show for the first time that eutrophication can alter the CO_2-equivalent balance of freshwater ecosystems in a non-linear way, and have a negative or a positive feedback on climate depending on the magnitude of productivity increase. In contrast, a recent study used exponential relationships between CO_2, CH_4 and Chl$a$ or TP to predict a future increase of freshwater CO_2-equivalent emission due to eutrophication (DelSontro et al., 2018). This difference in productivity and CO_2-equivalent emission relationships may arise from spatial disconnection of measurements; while our data describe the effect of productivity on the balance of CO_2 and CH_4, the other study used published data from different systems to derive separate relationships for CO_2 and CH_4, and can therefore not reflect any combined effect within a single ecosystem (Figure 4). The experimental evidence presented here calls for studies on natural systems that investigate both the CO_2 and CH_4 balance over a gradient of productivity, not the least since the thresholds between a negative to a positive feedback on climate are susceptible to differ between fresh water types and climatic zones.

DATA AVAILABILITY STATEMENT

The data that support the findings of this study are available from the corresponding author upon reasonable request.

ORCID

Charlotte Grasset https://orcid.org/0000-0002-3251-7974

REFERENCES

Anderson, N. J., Bennion, H., & Lotter, A. F. (2014). Lake eutrophication and its implications for organic carbon sequestration in Europe. *Global Change Biology*, 20(9), 2741–2751. https://doi.org/10.1111/gcb.12584

Atwood, T. B., Hammill, E., Greig, H. S., Kratina, P., Shurin, J. B., Srivastava, D. S., & Richardson, J. S. (2013). Predator-induced reduction of freshwater carbon dioxide emissions. *Nature Geoscience*, 6(3), 191–194. https://doi.org/10.1038/ngeo1734

Balmer, M. B., & Downing, J. A. (2011). Carbon dioxide concentrations in eutrophic lakes: Undersaturation implies atmospheric uptake. *Inland Waters*, 1(2), 125–132. https://doi.org/10.5268/IW-1.2.366

Barbosa, P. M., Farjalla, V. F., Melack, J. M., Amaral, J. H. F., da Silva, J. S., & Forsberg, B. R. (2018). High rates of methane oxidation in an Amazon floodplain lake. *Biogeochemistry*, 137(3), 351–365. https://doi.org/10.1007/s10533-018-0425-2

Bastviken, D. (2009). Methane. In G. E. Likens (Ed.), *Encyclopedia of inland waters* (pp. 783–805). Oxford, UK: Academic Press.

Bastviken, D., Cole, J. J., Pace, M. L., & Tranvik, L. (2004). Methane emissions from lakes: Dependence of lake characteristics, two regional assessments, and a global estimate. *Global Biogeochemical Cycles*, 18(4), GB4009. https://doi.org/10.1029/2004GB002238

Bastviken, D., Ejlertsson, J., & Tranvik, L. (2002). Measurement of methane oxidation in lakes: A comparison of methods. *Environmental Science & Technology*, 36(15), 3354–3361. https://doi.org/10.1021/es010311p

Bastviken, D., Tranvik, L. J., Downing, J. A., Crill, P. M., & Enrich-Prast, A. (2011). Freshwater methane emissions offset the continental carbon sink. *Science*, 331(6013), 50. https://doi.org/10.1126/science.1196808

Beaulieu, J., DelSontro, T., & Downing, J. (2019). Eutrophication will increase methane emissions from lakes and impoundments during the 21st century. *Nature Communications*, 10. https://doi.org/10.1038/s41467-019-09100-5

Benson, B. B., & Krause Jr., D. (1984). The concentration and isotopic fractionation of oxygen dissolved in freshwater and seawater in equilibrium with the atmosphere. *Limnology and Oceanography*, 29(3), 620–632. https://doi.org/10.4319/lo.1984.29.3.0620

Carpenter, S. R., Cole, J. J., Hodgson, J. R., Kitchell, J. F., Pace, M. L., Bade, D., … Schindler, D. E. (2001). Trophic cascades, nutrients, and lake productivity: Whole-lake experiments. *Ecological Monographs*, 71(2), 163–186. https://doi.org/10.2307/2657215

Cole, J. J., & Caraco, N. F. (1998). Atmospheric exchange of carbon dioxide in a low-wind oligotrophic lake measured by the addition of SF6. *Limnology and Oceanography*, 43(4), 647–656.

Cole, J. J., Pace, M., Carpenter, S., & Kitchell, J. (2000). Persistence of net heterotrophy in lakes during nutrient addition and food web manipulation. *Limnology and Oceanography*, 45, 1718–1730. https://doi.org/10.4319/lo.2000.45.8.1718

Cole, J. J., Prairie, Y. T., Caraco, N. F., McDowell, W. H., Tranvik, L. J., Striegl, R. G., … Melack, J. (2007). Plumbing the global carbon cycle: Integrating inland waters into the terrestrial carbon budget. *Ecosystems*, 10(1), 172–185. https://doi.org/10.1007/s10021-006-9013-8

Davidson, T. A., Audet, J., Jeppesen, E., Landkildehus, F., Lauridsen, T. L., Søndergaard, M., & Syväranta, J. (2018). Synergy between nutrients and warming enhances methane ebullition from experimental lakes. *Nature Climate Change*, 8(2), 156–160. https://doi.org/10.1038/s41558-017-0063-z

Davidson, T. A., Audet, J., Svenning, J.-C., Lauridsen, T. L., Søndergaard, M., Landkildehus, F., … Jeppesen, E. (2015). Eutrophication effects on greenhouse gas fluxes from shallow-lake mesocosms override those of climate warming. *Global Change Biology*, 21(12), 4449–4463. https://doi.org/10.1111/gcb.13062

DelSontro, T., Beaulieu, J. J., & Downing, J. A. (2018). Greenhouse gas emissions from lakes and impoundments: Upscaling in the face of global change. *Limnology and Oceanography Letters*, *3*(3), 64–75. https://doi.org/10.1002/lol2.10073

Devlin, S. P., Saarenheimo, J., Syväranta, J., & Jones, R. I. (2015). Top consumer abundance influences lake methane efflux. *Nature Communications*, *6*(1), 8787. https://doi.org/10.1038/ncomms9787

Duarte, C., & Prairie, Y. (2005). Prevalence of heterotrophy and atmospheric CO_2 emissions from aquatic ecosystems. *Ecosystems*, *8*, 862–870. https://doi.org/10.1007/s10021-005-0177-4

Flanagan, K. M., Mccauley, E., & Wrona, F. (2006). Freshwater food webs control carbon dioxide saturation through sedimentation. *Global Change Biology*, *12*(4), 644–651. https://doi.org/10.1111/j.1365-2486.2006.01127.x

Fuchs, A., Lyautey, E., Montuelle, B., & Casper, P. (2016). Effects of increasing temperatures on methane concentrations and methanogenesis during experimental incubation of sediments from oligotrophic and mesotrophic lakes. *Journal of Geophysical Research: Biogeosciences*, *121*(5), 1394–1406. https://doi.org/10.1002/2016JG003328

Grasset, C., Abril, G., Guillard, L., Delolme, C., & Bornette, G. (2016). Carbon emission along a eutrophication gradient in temperate riverine wetlands: Effect of primary productivity and plant community composition. *Freshwater Biology*, *61*(9), 1405–1420. https://doi.org/10.1111/fwb.12780

Grasset, C., Mendonça, R., Villamor Saucedo, G., Bastviken, D., Roland, F., & Sobek, S. (2018). Large but variable methane production in anoxic freshwater sediment upon addition of allochthonous and autochthonous organic matter. *Limnology and Oceanography*, *63*, 1488–1501. https://doi.org/10.1002/lno.10786

Hanson, P. C., Bade, D. L., Carpenter, S. R., & Kratz, T. K. (2003). Lake metabolism: Relationships with dissolved organic carbon and phosphorus. *Limnology and Oceanography*, *48*(3), 1112–1119. https://doi.org/10.4319/lo.2003.48.3.1112

Hanson, P. C., Pollard, A. I., Bade, D. L., Predick, K., Carpenter, S. R., & Foley, J. A. (2004). A model of carbon evasion and sedimentation in temperate lakes. *Global Change Biology*, *10*(8), 1285–1298. https://doi.org/10.1111/j.1529-8817.2003.00805.x

Heathcote, A. J., & Downing, J. A. (2012). Impacts of eutrophication on carbon burial in freshwater lakes in an intensively agricultural landscape. *Ecosystems*, *15*(1), 60–70. https://doi.org/10.1007/s10021-011-9488-9

Holopainen, I. J., & Pitkänen, A. K. (1985). Population size and structure of crucian carp (*Carassius carassius* (L.)) in two small, natural ponds in Eastern Finland. *Annales Zoologici Fennici*, *22*(4), 397–406.

Huttunen, J. T., Lappalainen, K. M., Saarijärvi, E., Väisänen, T., & Martikainen, P. J. (2001). A novel sediment gas sampler and a subsurface gas collector used for measurement of the ebullition of methane and carbon dioxide from a eutrophied lake. *Science of the Total Environment*, *266*(1), 153–158. https://doi.org/10.1016/S0048-9697(00)00749-X

Jeppesen, E., Peder Jensen, J., SØndergaard, M., Lauridsen, T., & Landkildehus, F. (2000). Trophic structure, species richness and biodiversity in Danish lakes: Changes along a phosphorus gradient. *Freshwater Biology*, *45*(2), 201–218. https://doi.org/10.1046/j.1365-2427.2000.00675.x

Kosten, S., Piñeiro, M., de Goede, E., de Klein, J., Lamers, L. P. M., & Ettwig, K. (2016). Fate of methane in aquatic systems dominated by free-floating plants. *Water Research*, *104*, 200–207. https://doi.org/10.1016/j.watres.2016.07.054

Lofton, D. D., Whalen, S. C., & Hershey, A. E. (2014). Effect of temperature on methane dynamics and evaluation of methane oxidation kinetics in shallow Arctic Alaskan lakes. *Hydrobiologia*, *721*(1), 209–222. https://doi.org/10.1007/s10750-013-1663-x

Lorenzen, C. J. (1968). Carbon/chlorophyll relationships in an upwelling area. *Limnology and Oceanography*, *13*(1), 202–204. https://doi.org/10.4319/lo.1968.13.1.0202

Maberly, S. C., Barker, P. A., Stott, A. W., & De Ville, M. M. (2013). Catchment productivity controls CO_2 emissions from lakes. *Nature Climate Change*, *3*(4), 391–394. https://doi.org/10.1038/nclimate1748

Marcé, R., Obrador, B., Morguí, J., Riera, J., López, P., & Armengol, J. (2015). Carbonate weathering as a driver of CO_2 supersaturation in lakes. *Nature Geoscience*, *8*(2), 107–111. https://doi.org/10.1038/ngeo2341

McCauley, E. (1984). The estimation of the abundance and biomass of zooplankton in samples. In J. A. Downing & F. H. Rigler (Eds.), *A manual on methods for the assessment of secondary productivity in fresh waters* (Vol. *17*, pp. 228–265). Oxford, UK: Blackwell.

Mendonça, R., Müller, R. A., Clow, D., Verpoorter, C., Raymond, P., Tranvik, L. J., & Sobek, S. (2017). Organic carbon burial in global lakes and reservoirs. *Nature Communications*, *8*(1), 1694. https://doi.org/10.1038/s41467-017-01789-6

Moss, B., Kosten, S., Meerhoff, M., Battarbee, R. W., Jeppesen, E., Mazzeo, N., … Scheffer, M. (2011). Allied attack: Climate change and eutrophication. *Inland Waters*, *1*(2), 101–105. https://doi.org/10.5268/IW-1.2.359

Myhre, G., Shindell, D., Bréon, F.-M., Collins, W., Fuglestvedt, J., Huang, J., … Zhang, H. (2013). Anthropogenic and natural radiative forcing. In T. F. Stocker, D. Qin, G.-K. Plattner, M. Tignor, S. K. Allen, J. Boschung, A. Nauels, Y. Xia, V. Bex, & P. M. Midgley (Eds.), *Climate change 2013: The physical science basis. Contribution of working group I to the fifth assessment report of the Intergovernmental Panel on Climate Change* (pp. 659–740). Cambridge, UK and New York, NY: Cambridge University Press.

Oliveira Junior, E. S., Temmink, R. J. M., Buhler, B. F., Souza, R. M., Resende, N., Spanings, T., … Kosten, S. (2019). Benthivorous fish bioturbation reduces methane emissions, but increases total greenhouse gas emissions. *Freshwater Biology*, *64*, 197–207. https://doi.org/10.1111/fwb.13209

Pace, M. L., Cole, J. J., Carpenter, S. R., Kitchell, J. F., Hodgson, J. R., Van de Bogert, M. C., … Bastviken, D. (2004). Whole-lake carbon-13 additions reveal terrestrial support of aquatic food webs. *Nature*, *427*(6971), 240–243. https://doi.org/10.1038/nature02227

Pacheco, F. S., Roland, F., & Downing, J. A. (2013). Eutrophication reverses whole-lake carbon budgets. *Inland Waters*, *4*(1), 41–48. https://doi.org/10.5268/IW-4.1.614

Penttinen, O. P., & Holopainen, I. J. (1992). Seasonal feeding activity and ontogenetic dietary shifts in 600 Crucian carp, *Carassius carassius*. *Environmental Biology of Fishes*, *33*(1–2), 215–221. https://doi.org/10.1007/bf00002566

Prairie, Y. T., Alm, J., Beaulieu, J., Barros, N., Battin, T., Cole, J., … Vachon, D. (2018). Greenhouse gas emissions from freshwater reservoirs: What does the atmosphere see? *Ecosystems*, *21*(5), 1058–1071. https://doi.org/10.1007/s10021-017-0198-9

R Core Team. (2016). *R: A language and environment for statistical computing*. Vienna, Austria: R Foundation for Statistical Computing. Retrieved from https://www.R-project.org/

Raymond, P. A., Hartmann, J., Lauerwald, R., Sobek, S., McDonald, C., Hoover, M., … Guth, P. (2013). Global carbon dioxide emissions from inland waters. *Nature*, *503*(7476), 355–359. https://doi.org/10.1038/nature12760

Rineau, F., Malina, R., Beenaerts, N., Arnauts, N., Bardgett, R. D., Berg, M. P., … Vangronsveld, J. (2019). Towards more predictive and interdisciplinary climate change ecosystem experiments. *Nature Climate Change*, *9*(11), 809–816. https://doi.org/10.1038/s41558-019-0609-3

Schindler, D. E., Carpenter, S. R., Cole, J. J., Kitchell, J. F., & Pace, M. L. (1997). Influence of food web structure on carbon exchange between lakes and the atmosphere. *Science*, *277*(5323), 248–251.

Schmitz, O. J., Raymond, P. A., Estes, J. A., Kurz, W. A., Holtgrieve, G. W., Ritchie, M. E., ... Wilmers, C. C. (2014). Animating the carbon cycle. *Ecosystems*, *17*(2), 344–359. https://doi.org/10.1007/s10021-013-9715-7

Schütz, H., Schröder, P., & Rennenberg, H. (1991). 2 – Role of plants in regulating the methane flux to the atmosphere. In H. A. Mooney, T. D. Sharkey, & E. A. Holland (Eds.), *Trace gas emissions by plants* (pp. 29–63). San Diego, CA: Academic Press.

Sepulveda-Jauregui, A., Hoyos-Santillan, J., Martinez-Cruz, K., Walter Anthony, K. M., Casper, P., Belmonte-Izquierdo, Y., & Thalasso, F. (2018). Eutrophication exacerbates the impact of climate warming on lake methane emission. *Science of the Total Environment*, *636*, 411–419. https://doi.org/10.1016/j.scitotenv.2018.04.283

Shelley, F., Ings, N., Hildrew, A. G., Trimmer, M., & Grey, J. (2017). Bringing methanotrophy in rivers out of the shadows. *Limnology and Oceanography*, *62*(6), 2345–2359. https://doi.org/10.1002/lno.10569

Sundh, I., Bastviken, D., & Tranvik, L. J. (2005). Abundance, activity, and community structure of pelagic methane-oxidizing bacteria in temperate lakes. *Applied and Environment Microbiology*, *71*(11), 6746–6752. https://doi.org/10.1128/aem.71.11.6746-6752.2005

Thottathil, S., Reis, P., Giorgio, P., & Prairie, Y. (2018). The extent and regulation of summer methane oxidation in northern lakes. *Journal of Geophysical Research: Biogeosciences*, *123*(10), 3216–3230. https://doi.org/10.1029/2018JG004464

Tranvik, L. J., Downing, J. A., Cotner, J. B., Loiselle, S. A., Striegl, R. G., Ballatore, T. J., ... Weyhenmeyer, G. A. (2009). Lakes and reservoirs as regulators of carbon cycling and climate. *Limnology and Oceanography*, *54*(6part2), 2298–2314. https://doi.org/10.4319/lo.2009.54.6_part_2.2298

Wang, H., Lu, J., Wang, W., Yang, L., & Yin, C. (2006). Methane fluxes from the littoral zone of hypereutrophic Taihu Lake, China. *Journal of Geophysical Research: Atmospheres*, *111*(D17). https://doi.org/10.1029/2005jd006864

Wanninkhof, R. (1992). Relationship between wind speed and gas exchange over the ocean. *Journal of Geophysical Research: Oceans*, *97*(C5), 7373–7382. https://doi.org/10.1029/92jc00188

Weiss, R. (1974). Carbon dioxide in water and seawater: The solubility of a non-ideal gas. *Marine Chemistry*, *2*, 203–215. https://doi.org/10.1016/0304-4203(74)90015-2

West, W. E., Coloso, J. J., & Jones, S. E. (2012). Effects of algal and terrestrial carbon on methane production rates and methanogen community structure in a temperate lake sediment. *Freshwater Biology*, *57*(5), 949–955. https://doi.org/10.1111/j.1365-2427.2012.02755.x

Yamamoto, S., Alcauskas, J. B., & Crozier, T. E. (1976). Solubility of methane in distilled water and seawater. *Journal of Chemical & Engineering Data*, *21*(1), 78–80. https://doi.org/10.1021/je60068a029

Yan, X., Xu, X., Ji, M., Zhang, Z., Wang, M., Wu, S., ... Liu, H. (2018). Cyanobacteria blooms: A neglected facilitator of CH_4 production in eutrophic lakes. *Science of the Total Environment*, *651*, 466–474. https://doi.org/10.1016/j.scitotenv.2018.09.197

Yvon-Durocher, G., Allen, A. P., Bastviken, D., Conrad, R., Gudasz, C., St-Pierre, A., ... del Giorgio, P. A. (2014). Methane fluxes show consistent temperature dependence across microbial to ecosystem scales. *Nature*, *507*(7493), 488–491. https://doi.org/10.1038/nature13164

Zhang, G., Yu, H., Fan, X., Ma, J., & Xu, H. (2016). Carbon isotope fractionation reveals distinct process of CH4 emission from different compartments of paddy ecosystem. *Scientific Reports*, *6*, 27065. https://doi.org/10.1038/srep27065

SUPPORTING INFORMATION

Additional supporting information may be found online in the Supporting Information section.